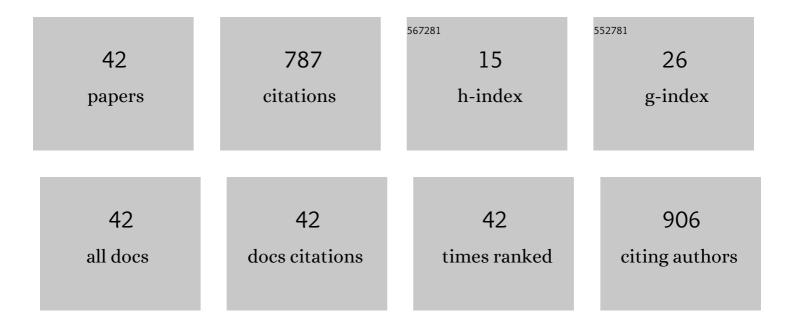
## Changfeng

List of Publications by Year in descending order

Source: https://exaly.com/author-pdf/1748402/publications.pdf Version: 2024-02-01



CHANCEENC

#	Article	IF	CITATIONS
1	Recent enhancement of central Pacific El Niño variability relative to last eight centuries. Nature Communications, 2017, 8, 15386.	12.8	126
2	Recent anthropogenic curtailing of Yellow River runoff and sediment load is unprecedented over the past 500 y. Proceedings of the National Academy of Sciences of the United States of America, 2020, 117, 18251-18257.	7.1	77
3	Anthropogenic Aerosols Cause Recent Pronounced Weakening of Asian Summer Monsoon Relative to Last Four Centuries. Geophysical Research Letters, 2019, 46, 5469-5479.	4.0	65
4	Effects of non-linear temperature and precipitation trends on Loess Plateau droughts. Quaternary International, 2015, 372, 175-179.	1.5	43
5	The 600-mm precipitation isoline distinguishes tree-ring-width responses to climate in China. National Science Review, 2019, 6, 359-368.	9.5	40
6	Asian Summer Monsoonâ€Related Relative Humidity Recorded by Tree Ring Î′ <sup>18</sup> O During Last 205 Years. Journal of Geophysical Research D: Atmospheres, 2019, 124, 9824-9838.	3.3	35
7	Elements content in tree rings from Xi'an, China and environmental variations in the past 30 years. Science of the Total Environment, 2018, 619-620, 120-126.	8.0	30
8	Tree-ring stable carbon isotope-based April–June relative humidity reconstruction since ad 1648 in Mt. Tianmu, China. Climate Dynamics, 2018, 50, 1733-1745.	3.8	25
9	Impacts of the superimposed climate trends on droughts over 1961–2013 in Xinjiang, China. Theoretical and Applied Climatology, 2017, 129, 977-994.	2.8	24
10	Drought severity and change in Xinjiang, China, over 1961–2013. Hydrology Research, 2017, 48, 1343-1362.	2.7	22
11	Regional difference of the start time of the recent warming in Eastern China: prompted by a 165-year temperature record deduced from tree rings in the Dabie Mountains. Climate Dynamics, 2018, 50, 2157-2168.	3.8	22
12	Growing-season precipitation since 1872 in the coastal area of subtropical southeast China reconstructed from tree rings and its relationship with the East Asian summer monsoon system. Ecological Indicators, 2017, 82, 441-450.	6.3	18
13	Tree-ring δ180 based PDSI reconstruction in the Mt. Tianmu region since 1618 AD and its connection to the East Asian summer monsoon. Ecological Indicators, 2019, 104, 636-647.	6.3	18
14	Sunshine duration reconstruction in the southeastern Tibetan Plateau based on tree-ring width and its relationship to volcanic eruptions. Science of the Total Environment, 2018, 628-629, 707-714.	8.0	17
15	Treeâ€ringâ€based precipitation reconstruction in the source region of Weihe River, northwest China since AD 1810. International Journal of Climatology, 2018, 38, 3421-3431.	3.5	16
16	Tree-ring evidence of the impacts of climate change and agricultural cultivation on vegetation coverage in the upper reaches of the Weihe River, northwest China. Science of the Total Environment, 2020, 707, 136160.	8.0	16
17	Tree-ring δ180, a tool to crack the paleo-hydroclimatic code in subtropical China. Quaternary International, 2018, 487, 3-11.	1.5	15
18	East Asian Summer Monsoon moisture sustains summer relative humidity in the southwestern Gobi Desert, China: evidence from δ180 of tree rings. Climate Dynamics, 2019, 52, 6321-6337.	3.8	15

CHANGFENG

#	Article	IF	CITATIONS
19	Climate Response of Tree Radial Growth at Different Timescales in the Qinling Mountains. PLoS ONE, 2016, 11, e0160938.	2.5	14
20	Delayed warming in Northeast China: Insights from an annual temperature reconstruction based on tree-ring δ180. Science of the Total Environment, 2020, 749, 141432.	8.0	13
21	A Picea crassifolia Tree-Ring Width-Based Temperature Reconstruction for the Mt. Dongda Region, Northwest China, and Its Relationship to Large-Scale Climate Forcing. PLoS ONE, 2016, 11, e0160963.	2.5	12
22	Tree-ring-based drought variability in the eastern region of the Silk Road and its linkages to the Pacific Ocean. Ecological Indicators, 2019, 96, 421-429.	6.3	11
23	Seasonal Palmer drought severity index reconstruction using tree-ring widths from multiple sites over the central-western Da Hinggan Mountains, China since 1825AAD. Climate Dynamics, 2019, 53, 3661-3674.	3.8	10
24	A 210-year tree-ring δ <sup>18</sup> O record in North China and its relationship with large-scale circulations. Tellus, Series B: Chemical and Physical Meteorology, 2022, 72, 1770509.	1.6	9
25	Effects of changing climate on reference crop evapotranspiration over 1961–2013 in Xinjiang, China. Theoretical and Applied Climatology, 2018, 131, 349-362.	2.8	8
26	An Asian Summer Monsoon-Related Relative Humidity Record from Tree-Ring δ180 in Gansu Province, North China. Atmosphere, 2020, 11, 984.	2.3	8
27	Oxygen stable isotopes of a network of shrubs and trees as high-resolution plaeoclimatic proxies in Northwestern China. Agricultural and Forest Meteorology, 2020, 285-286, 107929.	4.8	8
28	Evolution of the dry-wet variations since 1834 CE in the Lüliang Mountains, north China and its relationship with the Asian summer monsoon. Ecological Indicators, 2021, 121, 107089.	6.3	8
29	Temperature variation at the lowâ€katitude regions of East Asia recorded by tree rings during the past six centuries. International Journal of Climatology, 2020, 40, 1561-1570.	3.5	7
30	Changes in the Tree-Ring Width-Derived Cumulative Normalized Difference Vegetation Index over Northeast China during 1825 to 2013 CE. Forests, 2021, 12, 241.	2.1	7
31	Tree-ring width-based precipitation reconstruction in Zhaogaoguan, China since 1805 AD. Quaternary International, 2019, 510, 44-51.	1.5	6
32	Similarities and differences in driving factors of precipitation changes on the western Loess Plateau and the northeastern Tibetan Plateau at different timescales. Climate Dynamics, 2020, 55, 2889-2902.	3.8	6
33	Tree-ring-based drought variability in northern China over the past three centuries. Journal of Chinese Geography, 2022, 32, 214-224.	3.9	6
34	Interannual variability of average minimum temperatures derived from tree rings in the mid-Qinling Mountains, China, for the past 138Âyears. International Journal of Biometeorology, 2016, 60, 1519-1529.	3.0	5
35	Water Resource Management Implications for a Desert Oasis From Treeâ€Ring Î′ <sup>18</sup> 0 Variations in <i>Populus Euphratica</i> in Northwest China. Water Resources Research, 2022, 58, .	4.2	5
36	Maximum July–September temperatures derived from treeâ€ring densities on the western Loess Plateau, China. International Journal of Climatology, 2021, 41, 779-790.	3.5	4

CHANGFENG

#	Article	IF	CITATIONS
37	Relative humidity variation derived from treeâ€ring <scp>Î′<sup>18</sup>O</scp> and possible largeâ€scale atmospheric circulations linkage over the Guanzhong Plain, central northern China, since 1760 <scp>CE</scp> . International Journal of Climatology, 2021, 41, 3044-3057.	3.5	4
38	How is the El Niño–Southern Oscillation signal recorded by treeâ€ring oxygen isotopes in southeastern China?. International Journal of Climatology, 2022, 42, 6459-6478.	3.5	4
39	Ground surface temperature reconstruction for the Jinggangshan Mountains: Interpreting the hydro-thermal coupling pattern in southeastern China. Quaternary Science Reviews, 2020, 249, 106591.	3.0	3
40	Tree Rings Reveal the Impacts of the Northern Hemisphere Temperature on Precipitation Reduction in the Low Latitudes of East Asia Since 1259 CE. Journal of Geophysical Research D: Atmospheres, 2021, 126, e2020JD033603.	3.3	3
41	Recent intensification of hydroclimatic change in the middle reaches of the Yangtz River Basin driven by PDO, ENSO and WPSH. Climate Dynamics, 2022, 58, 1775-1790.	3.8	2
42	Temperature variations extracted from ring widths of firs growing in the humid environment of the mid-Qinling Mountains. Geografiska Annaler, Series A: Physical Geography, 2020, 102, 222-234.	1.5	0